

Figure S1. The radiomics model performances in the prediction of multiple molecular alterations. (A,B) The ROC curves for predicting target molecular status (positive-type and negative-type) in the validation set and testing set, respectively. (C,D) The ROC curves for predicting multiple mutations in the 8-panel cohort in the validation set and testing set, respectively. (E,F) The ROC curves for predicting multiple alterations in the 10-panel cohort in the validation set and testing set, respectively. (G,H) The ROC curves for predicting molecular expression in the subtype cohort in the validation set and testing set, respectively, EGFR_W and PD-L1- represent wild-type of EGFR and negative expression of PD-L1. PD-L1+ was separated into PD-L1+ Low and PD-L1+ High according to the TPS cutoff of 50%.

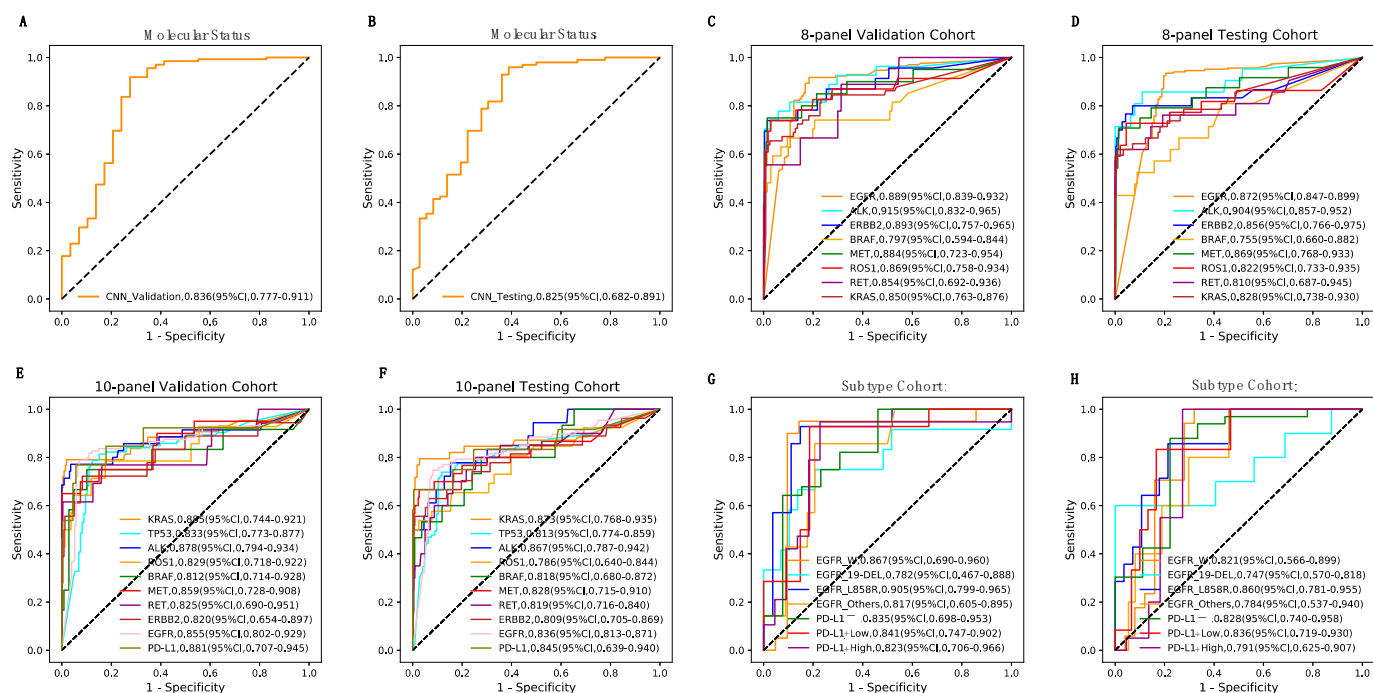


Figure S2. The CNN-based deep learning model performances in the prediction of multiple molecular alterations. (A,B) The ROC curves for predicting target molecular status (positive-type and negative-type) in the validation set and testing set, respectively. (C,D) The ROC curves for predicting multiple mutations in the 8-panel cohort in the validation set and testing set, respectively. (E,F) The ROC curves for predicting multiple alterations in the 10-panel cohort in the validation set and testing set, respectively. (G,H) The ROC curves for predicting molecular ex-pression in the subtype cohort in the validation set and testing set, respectively, EGFR_W and PD-L1- represent wild-type of EGFR and negative expression of PD-L1. PD-L1+ was separated into PD-L1+ Low and PD-L1+ High according to the TPS cutoff of 50%.

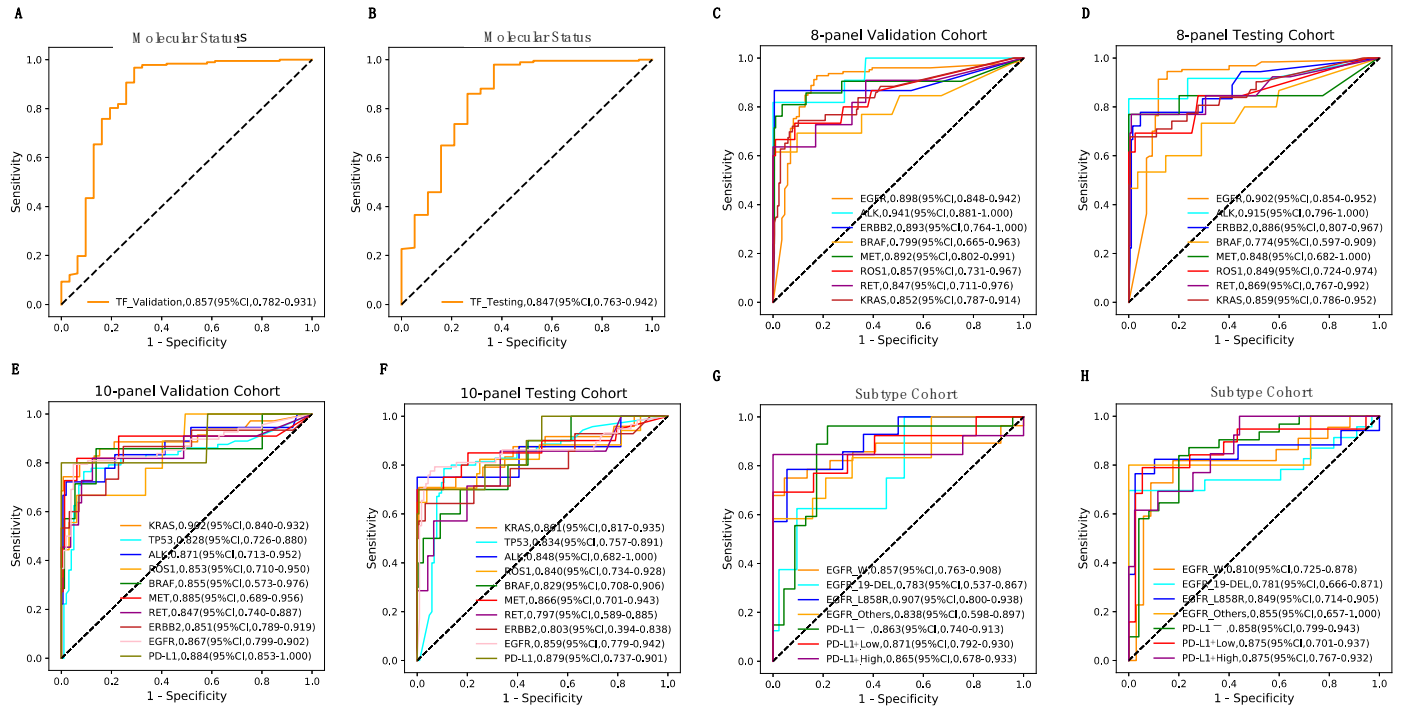


Figure S3. The transformer-based deep learning model performances in the prediction of multiple molecular alterations. (A,B) The ROC curves for predicting target molecular status (positive-type and negative-type) in the validation set and testing set, respectively. (C,D) The ROC curves for predicting multiple mutations in the 8-panel cohort in the validation set and testing set, respectively. (E,F) The ROC curves for predicting multiple alterations in the 10-panel cohort in the validation set and testing set, respectively. (G,H) The ROC curves for predicting molecular ex-pression in the subtype cohort in the validation set and testing set, respectively, EGFR_W and PD-L1- represent wild-type of EGFR and negative expression of PD-L1. PD-L1+ was separated into PD-L1+ Low and PD-L1+ High according to the TPS cutoff of 50%.

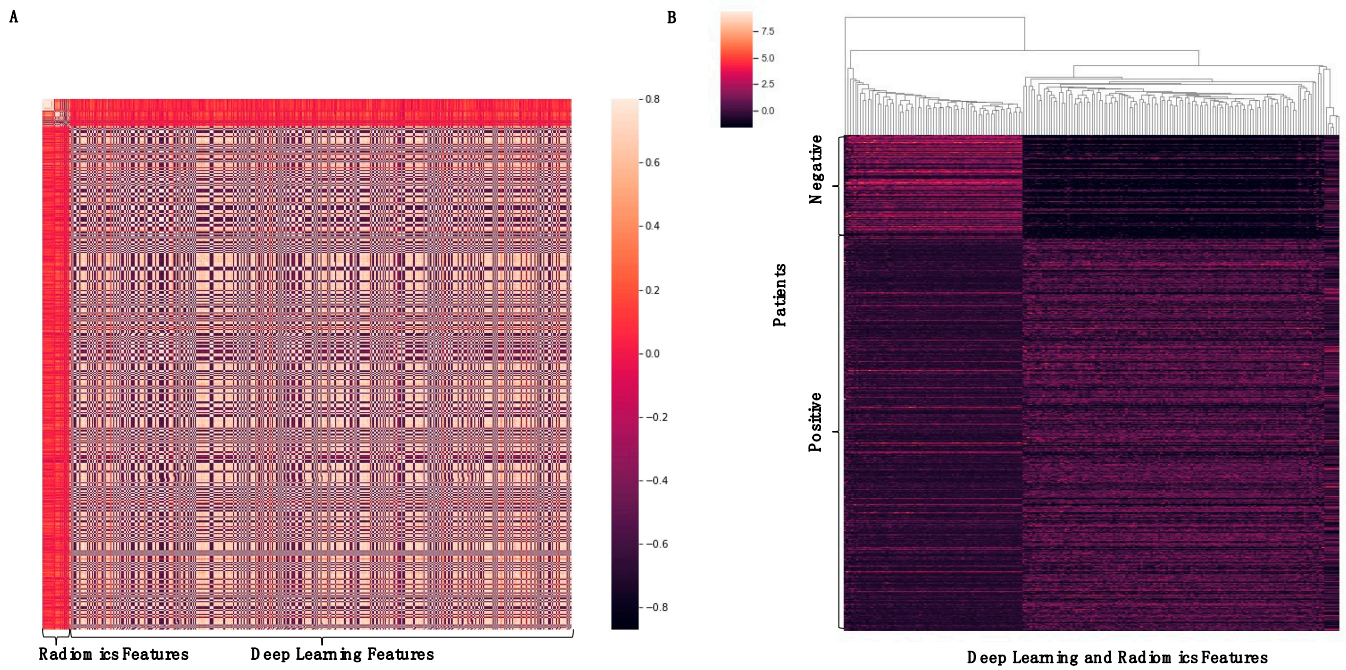


Figure S4. Association between radiomics and deep learning features. (A) Correlation heatmap of radiomics and deep learning features. (B) The correlation between selected features and the mutant genotypes patients in the development cohorts.

Table S1. The clinical characteristic of cancer shared dataset.

| | All Patients N = 1096 | 8-Panel Cohort N = 932 | 10-Panel Cohort N = 637 |
|-------------------|--------------------------|---------------------------|----------------------------|
| Age (SD) | 58.26 (10.69) | 58.11 (10.64) | 58.26 (11.03) |
| Sex | | | |
| Male | 598(54.6%) | 481(51.6%) | 393(61.7%) |
| Female | 498(45.4%) | 451(48.4%) | 244(38.3%) |
| Smoking history | | | |
| Current or former | 441(40.2%) | 346(37.1%) | 315(49.5%) |
| Never | 581(53.0%) | 525(56.3%) | 317(49.8%) |
| Unknow | 74(6.8%) | 61(6.5%) | 5(0.8%) |
| Histology type | | | |
| LUAD | 875(79.8%) | 786(84.3%) | 517(81.2%) |
| LUSC | 96(8.8%) | 48(5.2%) | 73(11.5%) |
| Others | 125(11.4%) | 98(10.5%) | 47(7.4%) |
| Actional mutation | | | |
| EGFR | | | |
| Mutant | 585(53.4%) | 585(62.8%) | 260(40.8%) |
| Wild | 511(46.6%) | 347(37.2%) | 377(59.2%) |
| ALK | | | |
| Mutant | 99(9.0%) | 99(10.6%) | 82(12.9%) |
| Wild | 997(91.0%) | 833(89.4%) | 555(87.1%) |
| ERBB2 | | | |
| Mutant | 82(7.5%) | 82(8.8%) | 63(9.9%) |
| Wild | 1014(92.5%) | 850(91.2%) | 574(90.1%) |
| BRAF | | | |
| Mutant | 43(3.9%) | 43(4.6%) | 34(5.3%) |
| Wild | 1053(96.1%) | 889(95.4%) | 603(94.7%) |

| | | | |
|-------------------------|-------------|------------|------------|
| <i>MET</i> | | | |
| Mutant | 74(6.8%) | 74(7.9%) | 61(9.6%) |
| Wild | 1022(93.2%) | 858(92.1%) | 576(90.4%) |
| <i>ROS1</i> | | | |
| Mutant | 43(3.9%) | 43(4.6%) | 37(5.8%) |
| Wild | 1053(96.1%) | 889(95.4%) | 600(94.2%) |
| <i>RET</i> | | | |
| Mutant | 46(4.2%) | 46(4.9%) | 38(6.0%) |
| Wild | 1050(95.8%) | 886(95.1%) | 599(94.0%) |
| <i>KRAS</i> | | | |
| Mutant | 140(12.8%) | 140(15.0%) | 116(18.2%) |
| Wild | 956(87.2%) | 792(85.0%) | 521(81.8%) |
| <i>TP53</i> | | | |
| Mutant | 315(28.7%) | - | 315(49.5%) |
| Wild | 322(29.4%) | - | 322(50.5%) |
| Unknown | 459(41.9%) | - | - |
| PD-L1 Expression | | | |
| Positive | 335 (30.6%) | - | 212(33.3%) |
| Negative | 432(39.4%) | - | 425(66.7%) |
| Unknown | 329(30.0%) | - | - |

Abbreviations: LUAD, lung adenocarcinoma; LUSC, lung squamous cell carcinoma.